Proceedings of the Fifth Annual LHCP
CMS-CR-2017/XXX
September 10, 2017

New results on Higgs properties

Jónatan Piedra

On behalf of the ATLAS and CMS Collaborations,
Instituto de Física de Cantabria
(CSIC - Universidad de Cantabria), Spain

ABSTRACT

We present the latest ATLAS and CMS measurements of several Higgs properties, such as signal-strength modifiers for the main production modes, fiducial and differential cross sections, and the Higgs mass. We have analyzed the 13 TeV proton-proton LHC collision data recorded in 2016, corresponding to integrated luminosities up to 36.1 fb^{-1}. Results for the $\text{H} \to \text{ZZ} \to 4\ell$ ($\ell = \text{e}\mu$), $\text{H} \to \gamma\gamma$, and $\text{H} \to \tau\tau$ decay channels are presented. In addition, searches for new phenomena in the $\text{H} \to \gamma\gamma + E_{\text{T}}^{\text{miss}}$ and $\text{H} \to \text{b}\overline{\text{b}} + E_{\text{T}}^{\text{miss}}$ decay channels are presented.

PRESENTED AT

The Fifth Annual Conference
on Large Hadron Collider Physics
Shanghai Jiao Tong University, Shanghai, China
May 15-20, 2017

1 Introduction

The discovery of the Higgs boson was announced in 2012 by the ATLAS and CMS collaborations [1, 2] based on proton-proton collisions collected at the CERN LHC at the centre of mass energies of 7 and 8 TeV. Since then a huge effort has been made in the determination of the properties of this newly found particle. The dataset already collected at 13 TeV allows inclusive Higgs boson measurements to be repeated. Furthermore, the increased centre-of-mass energy results in much larger cross sections for events at high partonic centre-of-mass energy. This implies improved sensitivity to a variety of interesting physics processes, such as Higgs bosons produced at high transverse momentum.

In this document we present the latest ATLAS and CMS measurements of several Higgs properties in different decay channels, such as $H \to ZZ$, $H \to \gamma\gamma$ and $H \to \tau\tau$. In addition, we also present results on searches for phenomena beyond the Standard Model, in Higgs decays to $\gamma\gamma$ or $b\bar{b}$, with E_T^{miss} in the final state.

2 H → ZZ

The $H \to ZZ \to 4\ell$ decay channel ($\ell = e, \mu$) has a large signal-to-background ratio due to the complete reconstruction of the final state decay products and excellent lepton momentum resolution, making it one of the most important channels for studies of the Higgs boson's properties. Here we present measurements of properties of the Higgs boson in this channel at 13 TeV, for both the ATLAS and CMS collaborations [3, 4].

In [4] the full kinematic information from each event using either the Higgs boson decay products or associated particles in its production is extracted with matrix element calculations, and used to form several kinematic discriminants. Both H boson decay kinematics and kinematics of associated production of H+jet, H+2 jets, VBF, ZH and WH are explored. In order to improve the sensitivity to the Higgs boson production mechanisms, the selected events are classified into mutually exclusive categories, based on jet multiplicity, b-tagged jets, the existence of additional leptons and the aforementioned kinematic discriminants. The reconstructed four-lepton invariant mass distribution is shown in Figure 1 (bottom left) for the sum of the 4e, 4μ and $2e2\mu$ subchannels. To extract the signal strength for the excess of events observed in the Higgs boson peak region a multi-dimensional fit is performed, on the four-lepton invariant mass and one of the kinematic discriminants. The fit is performed for several signal-strength modifiers controlling the contribution of the main SM Higgs boson production modes: ggH, VBF, WH, ZH and ttH, getting for all of them values consistent with the SM expectaction, as can be seen in Figure 2 (center). The inclusive observed signal-strength modifier is $1.05^{+0.15}_{-0.14}(\text{stat.})^{+0.11}_{-0.09}(\text{syst.})$. Two signal-strength modifiers $\mu_{ggH,ttH}$ and $\mu_{VBF,VH}$ are introduced as scale factors for the fermion and vector-boson induced contributions to the expected SM cross section. A two-dimensional fit is performed assuming a mass of $m_H = 125.09$ GeV leading to the measurements of $\mu_{ggH,ttH} = 1.20^{+0.35}_{-0.31}$ and $\mu_{VBF,VH} = 0.00^{+1.37}_{-0.00}$. The 68% and 95% CL contours are shown in Figure 2 (left). We have also measured the cross section for the production and decay $pp \to H \to 4\ell$ within a fiducial volume defined to closely match the reconstruction selection. The integrated fiducial cross section is measured to be $\sigma_{fid} 2.90^{+0.48}_{-0.44}(\text{stat.})^{+0.27}_{-0.22}(\text{syst.})$ fb. This can be compared to the SM expectation of 2.72 ± 0.14 fb. The measured differential cross section results for p_T^H and N_{jets} can also be seen in Figure 1 (bottom center and bottom right). The dominant sources of systematic uncertainty are the experimental uncertainties in the lepton identification efficiencies and luminosity measurement. In order to improve the four-lepton invariant mass resolution a 3D kinematic fit is performed using a mass constraint on the intermediate Z resonance. The simultaneous fit on the four-lepton invariant mass, the mass resolution and one of the kinematic discriminants gives $m_H = 125.26 \pm 0.20(\text{stat.}) \pm 0.08(\text{syst.})$ GeV. The Higgs width is also measured in the range $105 < m_{4\ell} < 140$ GeV. No assumptions need to be made about the presence of BSM particles or interactions which could affect the Higgs boson couplings either in production or in decay. We obtain a width that is constrained to be $\Gamma_H < 1.10$ GeV at 95% CL.

The ATLAS [3] four-lepton invariant mass can be seen in Figure 1 (top left). Similarly to the CMS analysis, fiducial cross sections are defined at particle-level, with a selection chosen to closely match the detector-level analysis. The inclusive fiducial cross sections of Higgs-boson production at 13 TeV measured using $H \to ZZ \to 4\ell$ decays are presented in Figure 2 (right). The fiducial cross section is measured to be

$3.62^{+0.53}_{-0.50}(\text{stat.})^{+0.25}_{-0.20}(\text{syst.})$ fb, in agreement with the SM prediction of 2.91 ± 0.13 fb. The measured total cross section is $69^{+10}_{-9}(\text{stat.})^{+5}_{-4}(\text{syst.})$ pb, to be compared with the SM prediction of 55.6 ± 2.5 pb. The measured differential cross sections for p_T^H and N_{jets}, together with their comparisons to SM predictions, are presented in Figure 1 (top center and right).

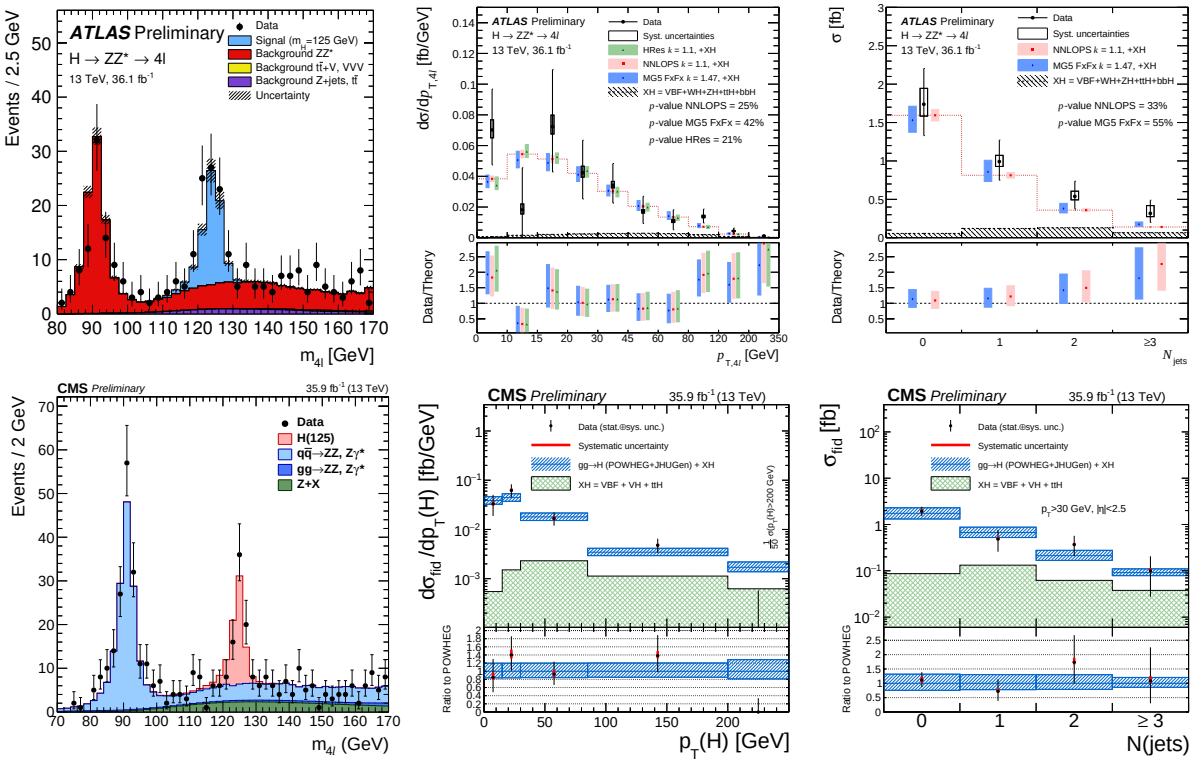

Figure 1: (Top left) ATLAS four-lepton invariant mass distribution of the selected events. The systematic uncertainty on the prediction is shown by the dashed band. (Top center and right) ATLAS differential fiducial cross sections, for the transverse momentum of the Higgs boson and the number of jets. The measured cross sections are compared to different ggH predictions, and predictions for all other Higgs production modes XH are added. (Bottom left) CMS four-lepton invariant mass distribution of the selected events. (Bottom center and right) CMS differential fiducial cross sections, for the transverse momentum of the Higgs boson and the number of jets. The sub-dominant component of the signal (VBF + VH + ttH) is denoted as XH.

3 $\mathbf{H \to \gamma\gamma}$

The Higgs boson decay into two photons ($H \to \gamma\gamma$) is a particularly attractive way to study the properties of the Higgs boson. Despite the small branching ratio, a reasonably large signal yield can be obtained thanks to the high photon reconstruction identification efficiencies at both ATLAS and CMS. Furthermore, the signal manifests itself as a narrow peak in the diphoton invariant mass spectrum on top of a smoothly falling background, and the Higgs boson signal yield can be measured using an appropriate fit.

In [5] the Higgs boson signal is measured through a maximum-likelihood fit to the diphoton invariant mass spectrum in the range $105 < m_{\gamma\gamma} < 160$ GeV for several fiducial regions, for each bin of the differential distributions, and for each event category used in extracting the production cross sections and signal strengths. The analysis is performed on 13.3 fb^{-1} at $\sqrt{s} = 13$ TeV, and the diphoton invariant mass for the inclusive data sample can be seen in Figure 3 (top left). These events are split into exclusive categories that are optimised for the best separation of the Higgs boson production processes. These categories are

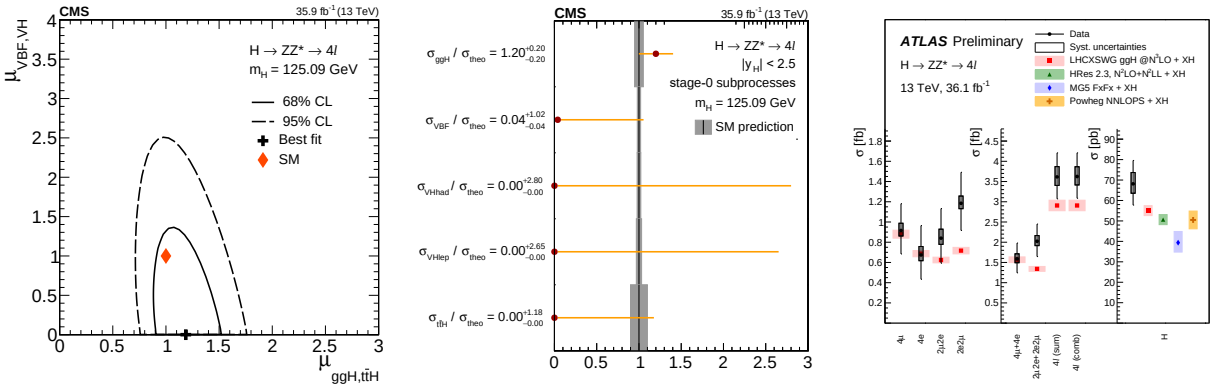

Figure 2: (Left) Result of the 2D likelihood scan for the $\mu_{\mathrm{ggH,ttH}}$ and $\mu_{\mathrm{VBF,VH}}$ signal-strength modifiers. The solid and dashed contours show the 68% and 95% CL regions, respectively. The cross indicates the best-fit values, and the diamond represents the expected values for the SM Higgs boson. (Center) Results of the fit for simplified template cross sections for the stage 0 sub-processes, normalized to the SM prediction. (Right) The fiducial cross sections and total cross section of Higgs-boson production measured in the 4ℓ final state. The SM prediction includes the N3LO calculation for ggH production.

ttH, VH, VBF, and untagged for the remaining events. This last category contains mostly events produced through gluon fusion. Several results are extracted from this analysis, starting with a fiducial cross section for $\mathrm{pp} \to \mathrm{H} \to \gamma\gamma$, measured to be $\sigma_{\mathrm{fid}} = 43.2 \pm 14.9(\mathrm{stat.}) \pm 4.9(\mathrm{syst.})$ fb, which is to be compared with the SM prediction for inclusive Higgs boson production of $62.8^{+3.4}_{-4.4}$ fb. The gluon fusion contribution to the SM prediction is N3LO. The differential cross sections for $\mathrm{pp} \to \mathrm{H} \to \gamma\gamma$ as a function of the diphoton transverse momentum and number of jets are shown in Figure 3 (top center and top right). The production mode event categories are used to determine simplified template cross sections and total production mode cross sections, as well as the corresponding signal strengths. In these fits, the cross sections of the bbH and tH production processes are fixed to the expected values from the SM. With the present dataset, the observed significance of the $\mathrm{H} \to \gamma\gamma$ signal is 4.7σ, while 5.4σ is expected for a SM Higgs boson. The corresponding signal strengths measured for the different production processes, and globally, are summarised in Figure 4 (Left), which also shows the global signal strength measured in Run-I.

In [6] and [7] CMS has measured the integrated and differential fiducial production cross sections for the Higgs boson in the diphoton decay channel, using 35.9 fb^{-1} of proton-proton collision data collected at $\sqrt{\mathrm{s}} = 13$ TeV. In Figure 3 (bottom left) the diphoton invariant mass is shown, and in Figure 3 (bottom center and right) the measurement of the differential cross section is reported as a function of the Higgs boson transverse momentum and the jet multiplicity. The fiducial cross section is measured to be $\sigma_{\mathrm{fid}} = 84 \pm 11(\mathrm{stat.}) \pm 7(\mathrm{syst.})$ fb, to be compared with the SM prediction of 75 ± 4 fb. This measurement is the most precise to date. We also report the overall signal strength, the rates for signal strengths $\mu_{\mathrm{VBF,VH}}$ and $\mu_{\mathrm{ggH,ttH}}$ for the model with these two parameters allowed to vary, and cross section ratios for the Stage 0 STXS process definitions, as shown in Figure 4 (right). The best fit signal strength obtained profiling $\mathrm{m_H}$ is reported to be $\mu = 1.16^{+0.11}_{-0.10}(\mathrm{stat.})^{+0.09}_{-0.08}(\mathrm{syst.})^{+0.06}_{-0.05}(\mathrm{theo.})$. The best-fit values for the signal strength modifiers associated with the ggH and ttH production mechanisms, and with the VBF and VH production processes are measured; the best fit values for each modifier are $\mu_{\mathrm{ggH,ttH}} = 1.19^{+0.20}_{-0.18}$ and $\mu_{\mathrm{VBF,VH}} = 1.01^{+0.57}_{-0.51}$. When μ_{ttH} is considered separately, the best-fit value is $\mu_{\mathrm{ttH}} = 2.2^{+0.9}_{-0.8}$, corresponding to a 3.3σ excess with respect to the absence of μ_{ttH} production, and compatible within 1.6σ with the SM μ_{ttH} prediction.

4 $\mathbf{H \to \tau\tau}$

To establish the mass generation mechanism for fermions, it is necessary to demonstrate the direct coupling of the scalar boson to fermions, and the proportionality of its strength to the fermion mass. The most

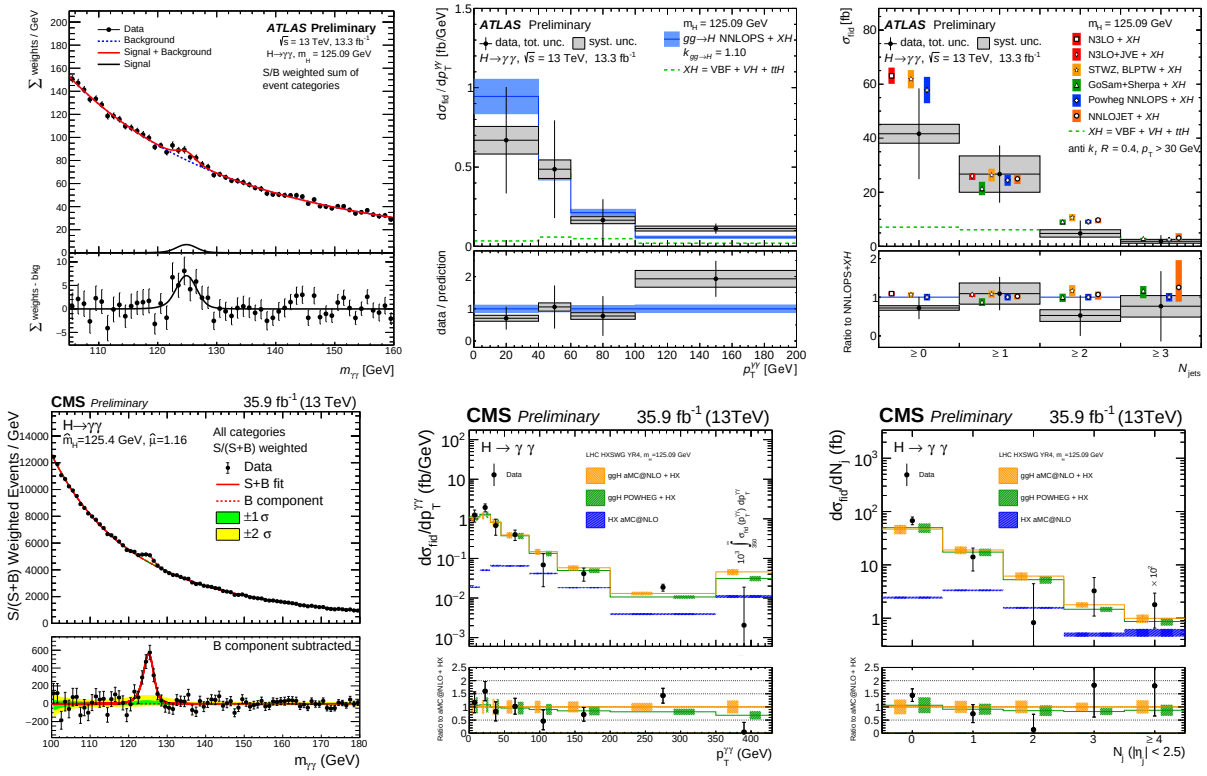

Figure 3: (Top left) ATLAS diphoton invariant mass spectrum. (Top center and right) ATLAS differential fiducial cross sections, for the transverse momentum of the Higgs boson and the number of jets. (Bottom left) CMS diphoton invariant mass spectrum. (Bottom center and right) CMS differential fiducial cross sections, for the transverse momentum of the Higgs boson and the number of jets.

promising decay channel is $\tau\tau$, because of the large event rate expected in the SM compared to the other leptonic decay modes, and of the smaller contribution from background events with respect to the $\mathrm{b\bar{b}}$ channel. Here we report the results of a search for the SM scalar boson using 35.9 fb^{-1} at 13 TeV, when it decays to a pair of τ leptons [8]. The four τ-pair final states with the largest branching fractions, $\mu\tau_{\mathrm{h}}$, $\mathrm{e}\tau_{\mathrm{h}}$, $\tau_{\mathrm{h}}\tau_{\mathrm{h}}$, and $\mathrm{e}\mu$, are studied.

The search for an excess of SM scalar boson events over the expected background involves a global maximum likelihood fit based on two-dimensional distributions in all channels, together with control regions for the $\mathrm{t\bar{t}}$, QCD multijet and W+jets backgrounds. Figure 5 shows the distribution observed, together with the expected background and signal distributions, in the $\tau_{\mathrm{h}}\tau_{\mathrm{h}}$ channel and VBF category. The signal prediction for a scalar boson with $m_{\mathrm{H}} = 125$ GeV is normalized to its best-fit cross section times branching fraction. The background distributions are adjusted to the results of the global maximum likelihood fit.

5 Searches for new phenomena

Many searches for dark matter (DM) at the LHC involve missing transverse momentum produced in association to detectable particles. Here we present an updated search by the ATLAS experiment [9] for DM associated with the SM Higgs boson decaying to a pair of photons using 36.1 fb^{-1} of pp collision data collected at 13 TeV. Three theoretical benchmark models are considered in this analysis. In the Z'_{B} model a massive vector mediator Z' emits a Higgs boson and subsequently decays to a pair of Dirac fermionic DM candidates. The Z'-2HDM model involves the Z' boson decaying to the Higgs boson and an intermediate heavy pseudoscalar boson A^0, which then decays to a pair of Dirac fermionic DM particles. The third model,

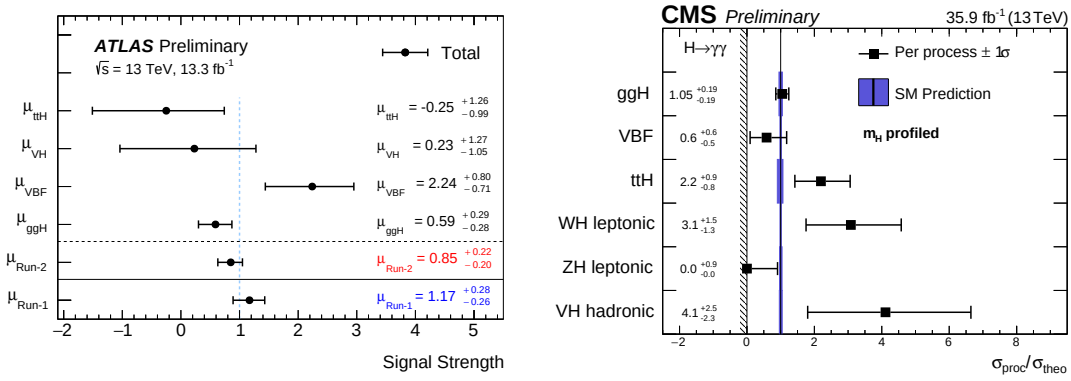

Figure 4: (Left) The ATLAS pp → H → γγ signal strength measured for the different production processes (ggH, VBF, VH and ttH) and globally, compared to the global signal strength measured at 7 and 8 TeV. The error bars show the total uncertainty. (Right) The CMS pp → H → γγ cross section ratios measured for each process (black squares) in the Higgs simplified template cross section framework, for profiled m_H, compared to the SM expectation and its uncertainties (blue band). The signal strength modifiers are constrained to be non-negative, as indicated by the vertical line and hashed pattern at zero.

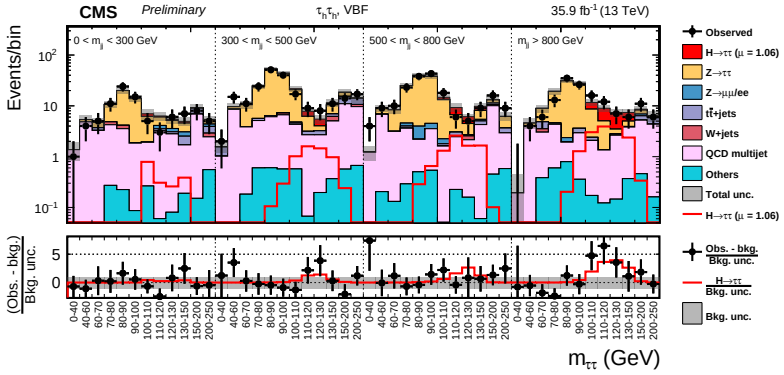

Figure 5: Observed and predicted 2D distributions in the VBF category of the $\tau_h\tau_h$ final state. The normalization of the predicted background distributions corresponds to the result of the global fit. The signal distribution is normalized to its best-fit signal strength.

referred to as the heavy scalar model, introduces a heavy scalar boson H produced primarily via gluon-gluon fusion. Here an effective quartic coupling between the SM Higgs h, H and two DM particles is considered, with the DM particle assumed to be scalar. The events that pass a common selection requiring at least two photon candidates are divided into five categories based on the event kinematics. These categories have been optimized based either on the Z'_B and Z′-2HDM signal samples, or using simulated heavy scalar boson samples, to cover the different kinematic regimes of the heavy scalar model. The results of the analysis are derived from a likelihood fit of the $m_{\gamma\gamma}$ distribution in the range of 105 GeV $< m_{\gamma\gamma} <$ 160 GeV. No significant excess over the background expectation is observed and 95% confidence level limits are set on the production cross section times branching fraction of the SM Higgs boson decaying into two photons in association with missing transverse energy in the three different theoretical benchmark models. 95% confidence level limits are also set on the observed signal strength in a two-dimensional m_χ-$m_{Z'_B}$ plane for the Z'_B model, and the m_{A^0}-$m_{Z'}$ plane for the Z′-2HDM model. In the model involving heavy scalar production, 95% confidence level upper limits are set on the production cross section times the branching fraction of H → hχχ, for a dark matter particle with mass of 60 GeV. The heavy scalar model is excluded for all the benchmark points investigated.

Another search for DM has been carried out in [10]. In this case DM is searched for in association with a SM-like Higgs boson decaying to a pair of b-quarks, using 36.1 fb^{-1} of pp collisions at 13 TeV recorded with the ATLAS detector. The Z′-2HDM model has been used for the optimization of the search and its interpretation. Multivariate algorithms are used to identify jets containing b-hadrons that are expected in $h \to b\bar{b}$ decays.

6 Conclusions

References

[1] G. Aad *et al.* [ATLAS Collaboration], Phys. Lett. B **716**, 1 (2012) [arXiv:1207.7214 [hep-ex]].

[2] S. Chatrchyan *et al.* [CMS Collaboration], Phys. Lett. B **716**, 30 (2012) [arXiv:1207.7235 [hep-ex]].

[3] G. Aad *et al.* [ATLAS Collaboration], ATLAS-HIGG-2016-25.

[4] CMS Collaboration [CMS Collaboration], CMS-PAS-HIG-16-041.

[5] G. Aad *et al.* [ATLAS Collaboration], ATLAS-CONF-2016-067.

[6] CMS Collaboration [CMS Collaboration], CMS-PAS-HIG-17-015.

[7] CMS Collaboration [CMS Collaboration], CMS-PAS-HIG-16-040.

[8] CMS Collaboration [CMS Collaboration], CMS-PAS-HIG-16-043.

[9] G. Aad *et al.* [ATLAS Collaboration], ATLAS-CONF-2017-024.

[10] G. Aad *et al.* [ATLAS Collaboration], ATLAS-CONF-2017-028.